

# Ab initio molecular dynamics simulation on the formation process of He@C<sub>60</sub> synthesized by explosion

Jian-Ying Li · Li-Min Liu · Bo Jin · Hua Liang ·  
Hai-Jun Yu · Hong-Chang Zhang · Shi-Jin Chu ·  
Ru-Fang Peng

Received: 28 October 2012 / Accepted: 13 December 2012 / Published online: 8 January 2013  
© Springer-Verlag Berlin Heidelberg 2013

**Abstract** The applications of endohedral non-metallic fullerenes are limited by their low production rate. Recently, an explosive method developed in our group shows promise to prepare He@C<sub>60</sub> at fairly high yield, but the mechanism of He inserting into C<sub>60</sub> cage at explosive conditions was not clear. Here, ab initio molecular dynamics analysis has been used to simulate the collision between C<sub>60</sub> molecules at high-temperature and high-pressure induced by explosion. The results show that defects formed on the fullerene cage by collision can effectively decrease the reaction barrier for the insertion of He into C<sub>60</sub>, and the self-healing capability of the defects was also observed.

**Keywords** Ab initio molecular dynamics · Collision · Explosion · He@C<sub>60</sub>

## Introduction

Endohedral fullerenes have received great attention because of their application in many fields such as pharmacy [1], quantum computing [2], materials science [3–5], etc. The inner space of fullerene is suitable to entrap small atoms or clusters [6], especially metallic atoms [7]. It is difficult to synthesize noble atom encapsulated fullerenes, because the reaction force between the cage and the atoms is too small to stabilize the complex [6, 8]. So far, some endohedral non-metallic fullerenes have been synthesized by different methods but with low yields of 0.4 % to 1 % [8–15].

The ability to perform a “molecular surgery”, which involves the open and close of the fullerene, may provide a new approach toward the encapsulation of certain atoms during the open process. A successful example is that Kei Kurotobi et al. has entrapped H<sub>2</sub>O and H<sub>2</sub> into C<sub>60</sub> by molecular surgical approach [12, 15]. On the other hand, ion bombardment technique can also break the C<sub>60</sub> cage to facilitate the insertion of He, Ne and other atoms [16, 17]. However, neither of the above two methods could closely meet the requirements of both high yield and high efficiency. Obviously, the main reason of the low yield for noble atoms comes from the high reaction barrier to penetrate the C<sub>60</sub> cage. Ohtsuki et al. suggested that it needs 130 eV for Xe and 80 eV for Kr to insert into C<sub>60</sub> through the six-membered ring [18]. In the case of He insertion into C<sub>60</sub>, generally the energy needed for penetration is around 8.7 to 12 eV [19–21]. For instance, tight-binding approach by Granot indicated that the kinetic energy of He penetrating C<sub>60</sub> need at least 12 eV [21]. For Patchkovskii’s calculations 8.7 eV barrier is obtained by semiempirical, ab initio and density functional [19], but the related energy barrier may be expected to be larger than 10 eV by the biased transition path sampling approach from molecular-dynamics simulation [20]. Recently, Peng et al. have successfully prepared He@C<sub>60</sub> at the yield of 4 % through an explosive method

---

J.-Y. Li · B. Jin · H. Liang · H.-J. Yu · H.-C. Zhang ·  
R.-F. Peng (✉)  
State Key Laboratory Cultivation Base for Nonmetal Composites  
and Functional Materials, Southwest University of Science and  
Technology, Mianyang, Sichuan 621010, China  
e-mail: rfpeng2006@163.com

J.-Y. Li · L.-M. Liu  
Beijing Computational Science Research Center, Beijing 100084,  
People’s Republic of China

S.-J. Chu  
Institute of Chemical Materials, Chinese Academy  
of Engineering Physics, Mianyang, Sichuan 621900, China  
e-mail: chushijin@swust.edu.cn

L.-M. Liu  
Chengdu Green Energy and Green Manufacturing Technology  
R&D Center, Chengdu 610207, Sichuan, China  
e-mail: limin.liu@csrc.ac.cn

(EM) [22]. This method possesses the merits of timely efficient and cost-effective, but the explosive process and mechanism are rather complex, which are extremely difficult to be modeled with a comprehensive and systematic solution. Moreover, the obscure reaction mechanism makes it rather difficult to adjust the experimental parameters, which forbids further improvement of the reaction efficiency.

To solve the bottle-neck problem, ab initio molecular dynamics (AIMD) simulation has been carried out in this paper to investigate the collision of  $C_{60}$  at atomic level and the formation process of  $He@C_{60}$  synthesized by EM. We suggest that if the defects on  $C_{60}$  cage are formed by losing carbon atoms, the traveling of He atoms in and out of the  $C_{60}$  cage becomes viable with a much lower barrier of 3.0 eV. Further studies show that the collisions between  $C_{60}$  molecules driven by explosion plays a crucial role in facilitating the formation of those defect. Besides, after He inserts into  $C_{60}$ , the defects can self-heal at the explosive environments.

## Experimental and theoretical details

In the previous experiments based on EM [22],  $C_{60}$  powder (150 mg, >99.9 %) and explosive of HMX (cyclic- $[CH_2N-NO_2]_4$ , 1 g) was initially put into the experiment apparatus at ca. 0.6 atm He. After detonation, the nearly instantaneous explosion produced a shock wave that accelerated He and  $C_{60}$  molecules collision in the experiment apparatus because of their extremely high speeds. Meanwhile, the temperature reached up to 2000–5000 K and pressure raised to 10–30 GPa in  $10^{-6}$ – $10^{-7}$  s [23]. These shock velocities came from HMX or RDX are typically from 4 to  $9 \times 10^3$  m  $s^{-1}$  by theoretical calculation [24–26]. To experimentally study explosion shock wave, a method of small scale gap test was improved to guarantee the steady propagation of shock wave, a Mn-Cu manometer was used to measure the detonation pressure (23.5–28.8 GPa), and the range of detonation velocity was 2 to  $5 \times 10^3$  m  $s^{-1}$ .

AIMD simulation within the framework of density functional theory (DFT) implemented in the CP2K/Quickstep package was carried out to stimulate the collision of fullerenes for the  $He@C_{60}$  synthesized [27–29]. CP2K/Quickstep package is based on the hybrid Gaussian and plane wave method. The Gaussian functions which consisted of a double- $\zeta$  plus polarization (DZP) basis set were employed to optimize the molecules structure. The energy cutoff for the real space grid used to represent the density was 320 Ry. Perdew, Burke and Ernzerhof (PBE) exchange-correlation functions [30] were used to simulate the collision between two  $C_{60}$  molecules. For some cases, the exchange correction of Becke and the correlation function of Lee, Yang and Parr (BLYP), local density approximation (LDA) and PBE plus

van der Waals dispersion corrections (PBE-vdw) [31] were also used to calculate the interaction energy between He and  $C_{60}$ . In our AIMD simulation, we carried out with the initial speeds of the molecules in the range of  $2.32 \times 10^3$  and  $3.28 \times 10^3$  m  $s^{-1}$ , as mentioned above. We determined the energy of the potential barrier for He inserts into  $C_{60}$  (and  $C_{58}$ ) using the climbing image nudged elastic band (NEB) method [32, 33]. In the NEB method, a set of images ( $N=12$ ) is uniformly distributed along the reaction path connecting the initial and final states optimized in our simulation. To ensure the continuity of the reaction path, the images are coupled with elastic forces, and each intermediate state is fully relaxed in the hyperspace perpendicular to the reaction coordinate [33].

## Results and discussion

### Theoretical analysis: interaction energy of $HeC_{60}$

We investigated the interaction of He with  $C_{60}$ . To determine the preferred site of He on  $C_{60}$  surface, we first calculated the interaction energy of  $HeC_{60}$  by placing the He atom on the pentagonal, hexagonal sites, carbon-carbon bond and a carbon atom, wherein the atom moved inward speeding up in the shock waves. It was an important step in the formation process of  $He@C_{60}$ . Here, the interaction energy of them is defined as follows:

$$E_{\text{com}} = E_{\text{HeC}_{60}} - (E_{\text{C}_{60}} + E_{\text{He}}), \quad (1)$$

where  $E_{\text{com}}$  is the interaction energy compared with various exchange-correlation functions,  $E_{\text{HeC}_{60}}$  is the total energy of fullerenes complex,  $E_{\text{C}_{60}}$  and  $E_{\text{He}}$  are the total energy of a free molecule He and  $C_{60}$ , respectively. We calculate the formation energies of He and  $C_{60}$  through PBE, PBE-vdw, BLYP, BLYP-vdw and PADE exchange-correlation functional, the He and  $C_{60}$  cage was obtained using the optimizations of the atomic geometries.

The results show that the interaction energy between He and  $C_{60}$  is about 0.01–0.04 eV with our calculation, where the interaction energy is found for a distance of 3.40 Å of the He from the  $C_{60}$  surface, which is in agreement with earlier calculations [34]. The results show a weak attractive interaction between them, it means there are many possibilities for the geometry of He and  $C_{60}$  complex because they nearly remain isolated from each other. We consider the geometry of He and  $C_{60}$  as this corresponds to the experiment apparatus, a question that need to be answered is as follows: how does He get into  $C_{60}$  in the shock wave, through a hexagonal (C6) or pentagonal (C5) of the perfect  $C_{60}$ ?

Energy barrier of the formation process of He@C<sub>60</sub>

There are two kinds of rings on C<sub>60</sub> cage, C5 and C6. Obviously, C6 has larger space for He to insert than C5 and other sites of C<sub>60</sub>, thus we mainly consider how He inserts into C<sub>60</sub> through C6.

Figure 1 shows that the reaction experiences for He insert into C<sub>60</sub> through the center of a C6 perpendicularly, which was explored with NEB method. The initial and final states correspond to He staying outside and inside C<sub>60</sub> as shown in Fig. 1a and c, respectively. The transition state is that one He atom inlaid within the C6, as a result of the cage deformed considerably, which can be seen in Fig. 1b. The lengths of C-C bonds are greatly increased by 0.1 and 0.2 Å relative to perfect C6, and the computed barrier for He inserting is 9.7 eV. The C6 restore its previous state after He goes into C<sub>60</sub> as we can see in Fig. 1c.

In this case, the He penetrates into the cage through the center of the C6 with difficulty, since the atom radius of He is 0.31 Å, the hole of a C6 is not large enough for He to be in and out of the C<sub>60</sub> cage freely. Thus the main energy barrier for He inserting into C<sub>60</sub> is used to enlarge the origin C6.

Such a large barrier greatly hampers the inserting process of He into C<sub>60</sub> and this should be the main reason that the production yield is rather low in most of the experimental studies [16, 17]. That is, it does not provide a direct penetration of a He through the center of a C6 occurs with suitably high kinetic energy in the explosion.

As mentioned above, both He and C<sub>60</sub> will be accelerated by the shock wave in the experimental conditions, thus they have great chance to collide together in a very short time, and the original C<sub>60</sub> may generate all kinds of defects in such processes because of the collision. In order to check whether the defect of C<sub>60</sub> can lower the reaction barrier and enhance the production yield, the reaction barrier of He inserting into C<sub>60</sub> with defect was also studied. Divacancy may be generated either by collision of C<sub>60</sub> or high-pressure and high temperature [35]. For such calculations, the typical defect and divacancy are used to study the reaction barrier.

As we know, C<sub>60</sub> is generally known to undergo consecutive C2 eliminations in what used to be called the Rice

shrink-wrap mechanism [36]. That means C<sub>58</sub>, C2 eliminations on C<sub>60</sub>, contains two kinds of ring, one is a 7-membered ring (C7) and the other is an 8-member ring (C8). C8 has a relative larger space than C6, thus it may be easier for He to pass through C8 than C6. To more accurately simulate process of He insert into C<sub>58</sub> through C7 and C8, the C<sub>60</sub> expel C2 unit and undergo cage shrinking was simulated in AIMD, The unimolecular dissociation channels for C<sub>60</sub> is shown in Eq. (2):



The structure of C<sub>58</sub> contains C7 when C<sub>60</sub> expel C2 unit in the adjacent hexagon, or contains C8 when C<sub>60</sub> expel C2 unite in the adjacent pentagon (see Fig. 2b and c).

As shown in Fig. 2a and d, in the perfect C<sub>60</sub>, the energy calculations showed that the He penetrates through the center of the C6 with a large energy of 9.75 eV. and the barriers for He inserting into C<sub>58</sub> are 5.36 and 3.00 eV for C7 and C8 (Fig. 2b, c and d), respectively. Compared with the energy 9.75 eV for He inserting into perfect fullerene, the divacancy on the fullerene can effectively lower the reaction barrier. That is to say, He@C<sub>60</sub> can be more easily fabricated from the fullerene with defect than the perfect.

C<sub>60</sub> collisions caused by shock wave

To further reveal the formation mechanism of He@C<sub>60</sub> at explosive condition, we simulate C<sub>60</sub> collision in the shock wave condition. The contact point and position of the initial structures of two C<sub>60</sub> did not describes in the model of collision. C<sub>60</sub> is based on one-dimension face-to-face collision under shock wave condition as mentioned by Jakowski et al. [37], namely, kinetic energy (or the velocities of the molecules) will be a major factor in deciding the final structures. It is suggest that the simulation provides a realistic way to depict the highly complex molecules collision in the experiment apparatus.

Under the explosive condition, a very high speed was imposed on C<sub>60</sub> by shock wave of HMX. C<sub>60</sub> molecules from opposite directions have a great chance to collide with each other at very high speed. In the process of collision,

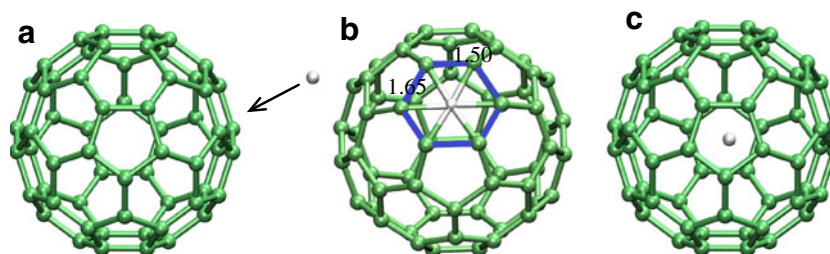
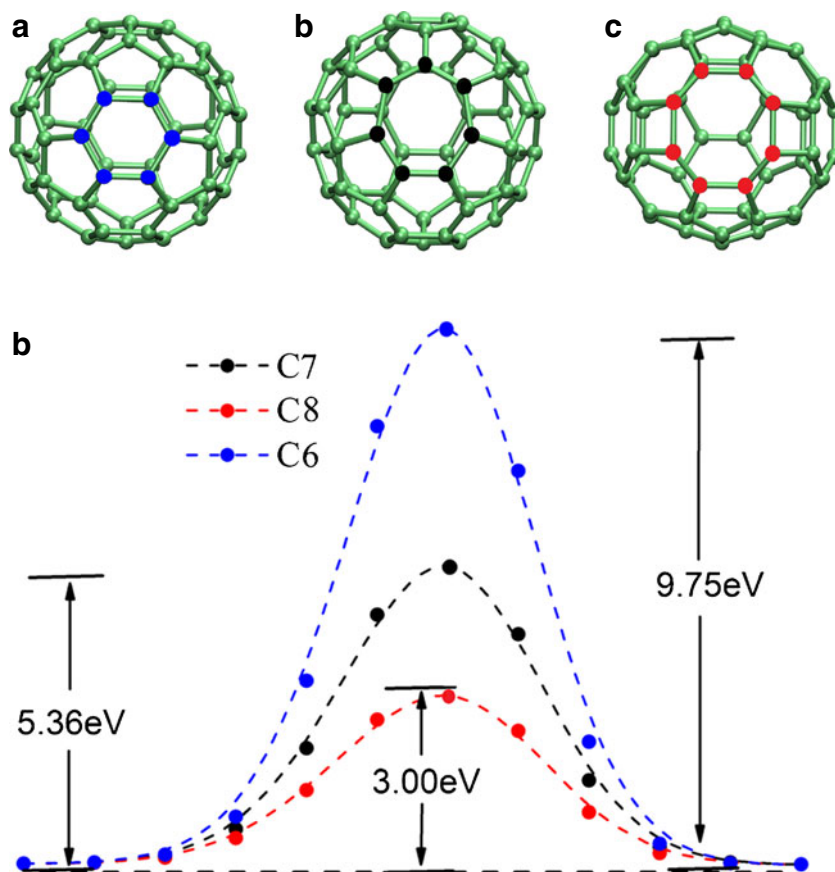


**Fig. 1** The reaction path for He inserting into C<sub>60</sub> through C6 by NEB method. **a** the initial state of He staying outside of C<sub>60</sub> and the arrow is the path of He to be inserted into C<sub>60</sub> through a C6, **b** the transition

state of He atom inlaid in a C6 and the bond length of the C6 increased from 1.41 to 1.50 and 1.45 to 1.65 Å, **c** the final state of He@C<sub>60</sub>

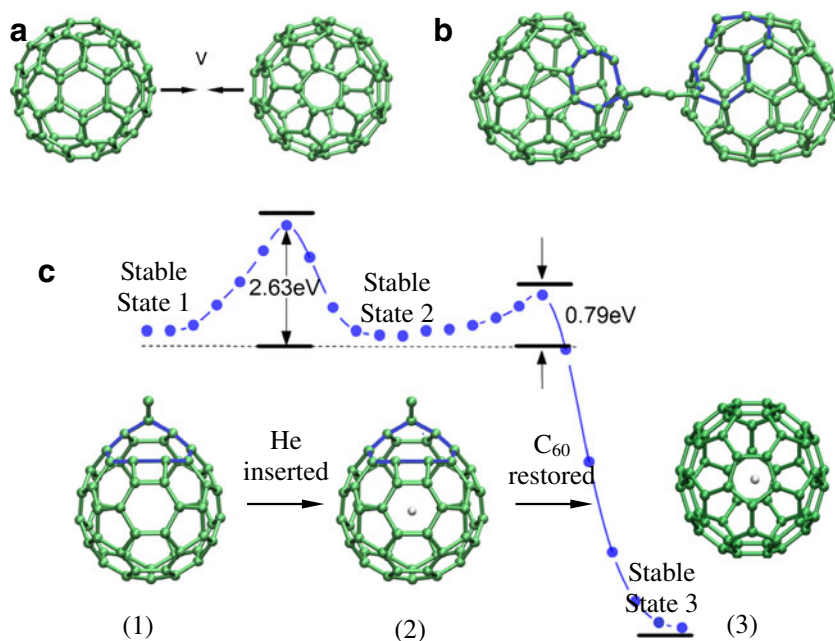
**Fig. 2** The energy barrier for He inserting the  $C_{60}$  and  $C_{58}$ . **a**, **b**, **c** show the atomic structure of C6 on  $C_{60}$ , and C7, C8 on  $C_{58}$  respectively. **d** shows the energy barriers for the He insert into the fullerenes through C6, C7 and C8



defects may be formed on some  $C_{60}$  cages. In order to understand the detailed information of  $C_{60}$  collision, several AIMD simulations were carried out with different initial speeds in the range of  $2.32 \times 10^3$  to  $3.28 \times 10^3$  m s<sup>-1</sup>. The AIMD results show that when the initial

speed of  $C_{60}$  is lower than  $2.59 \times 10^3$  m s<sup>-1</sup>, the  $C_{60}$  will bounce quickly, and no reaction occurs after this process. When the initial speeds of  $C_{60}$  are higher than  $3.00 \times 10^3$  m s<sup>-1</sup>, the two  $C_{60}$ s collide to form defects on their cages.

**Fig. 3** The structural evolution of an orifice in the collision with a velocities ( $V$ ) and encapsulation of He to open-cage  $C_{60}$ . **a** Initial structures of two  $C_{60}$  molecules, **b** a C9 and C11 orifice of an open-cage  $C_{60}$  dimer was formed, **c** the minimum energy reaction barrier path of He inserting into  $C_{60}$  cage through a C9 orifice and restoration of the orifice for synthesis of He@ $C_{60}$ . (1), (2), (3) show the stable states in the path for He insert into the  $C_{60}$ , through C9



AIMD simulation with the collision kinetic energy of 40 eV ( $3.28 \times 10^3 \text{ m s}^{-1}$ ) shows the collision-induced reactive case in Fig. 3. Figure 3a shows the initial structures of two  $C_{60}$  molecules face-to-face collision under shock wave condition. In our simulation, a pentagonal bond is first broken, and then a series of C-C bonds are broken and reorganization occurred, which lead to one of  $C_{60}$  opening a window. The orifice becomes larger because two pentagonal bonds are broken. A C11 of  $C_{60}$  dimer was formed in such process as shown in Fig. 3b. Although the C11 of the dimer is a transition state, considering window mechanisms, the transition structures for the passage of He through C11 windows needs to be verified. As a matter of fact, the dimer was easily separated by the collision of other fullerenes and molecule (e.g., C, NO,  $\text{NO}_2$  from explosion) in explosive atmosphere. The binding energy of the dimer separation is 6.8 eV as an independent molecule.

Similarly, in order to realize the C11 windows of an independent molecule, the molecular geometries were fully optimized. Ultimately, both of the  $C_{60}$ s were evolution of an orifice with C9 (shown in Fig. 3c).

AIMD simulations show that  $C_{60}$  will form defects during the collision process in the explosive conditions. Such results agree with Brink's experiment on endohedral fullerene collision which also suggests a large hole formation on fullerene cage [38] and shown by chemical method [11].

Figure 3c shows the stable states for the passage of He through C9 have been located and fully characterized at the PBE level, the He insertion with 2.63 eV shows that the energy barrier is obviously lower than the perfect  $C_{60}$ . Compared with the atom structure with the perfect  $C_{60}$ , only the C-C bonds of C6 are extended, thus the small structure change should be the main reason for the lower energy barrier for the He inserting into  $C_{60}$  during the collision. Saunders et al. have studied that the He release from the  $C_{60}$  with an energy barrier of 0.99~3.5 eV through an opened window in a fullerene on experimental work [11, 39], which would be in agreement with our calculation in such explosive conditions. Consequently, a defect formed by carbon atoms loss from the  $C_{60}$  can lower the reaction barrier and improve the productive yield for  $\text{He}@C_{60}$ . In addition, the orifice of C9 can easily restore to the perfect one with a barrier of 0.79 eV as shown in Fig. 3c.

As we can see, the shock wave from the explosion can not make the He insert into the perfect  $C_{60}$  directly, it may be limited by the kinetic energy of the He. Instead of this, opening an orifice on the  $C_{60}$  by collisions between molecules under the explosions was the main reason to get the high yields of  $\text{He}@C_{60}$ . It suggests that the formation process of  $\text{He}@C_{60}$  can be separated into three key steps. The first step is C-C bonds breaking and the defect forming through collision process of  $C_{60}$  molecules, and this step is the most important step. The second step is He inserting into  $C_{60}$  through the defect and the last step is the self-restoration

of the cage. The whole reaction mechanism mimics the self-healing method.

## Conclusions

AIMD simulations have been carried out to explore at the atomic level the formation process of  $\text{He}@C_{60}$  synthesized by EM. Although  $\text{He}@C_{60}$  can be generated through a direct inserting process, the rate is very low considering that the reaction barrier is rather high (about 10 eV). Our results show that the  $\text{He}@C_{60}$  can easily be formed by means of inserting He into  $C_{60}$  through opening an orifice on the cage. The main reason is that the EM can generate defected  $C_{60}$  in a very short time through collisions between  $C_{60}$  molecules, and He can be quickly inserted into the defected  $C_{60}$ . After such processes, the defected cages can be restored by other C atoms to form  $\text{He}@C_{60}$  in the atmosphere. Our results suggested that He inserting into  $C_{60}$  by EM is by a "window" mechanism. Such result paves an important way in understanding the formation process of  $\text{He}@C_{60}$  at explosive atmosphere.

**Acknowledgments** We are grateful for financial support from the National Natural Science Foundation of China (Project NOs. 50972122, 11244001, 51222212), Youth Innovation Research Team of Sichuan for Carbon Nanomaterials (Project No. 2011JTD0017), state key laboratory cultivation base for nonmetal composites and functional materials, Southwest University of Science and Technology (Project NO. 11ZXFK16) and Science Foundation of China Academy of Engineering Physics (Project NO. 11ZH0157).

## References

- Ball P (2011) Material witness: caged water. *Nat Mater* 10:649–649. doi:10.1038/nmat3107
- Ju CY, Suter D, Du JF (2007) Two-qubit gates between noninteracting qubits in endohedral-fullerene-based quantum computation. *Phys Rev A* 75:12318–12322
- Cimpoesu F, Ito S, Shimotani H, Takagi H, Dragoie N (2011) Vibrational properties of noble gas endohedral fullerenes. *Phys Chem Chem Phys* 13:9609–9615
- Saunders M, Jiménez-Vázquez HA, Cross RJ, Mroczkowski S, Freedberg DI, Anet FAL (1994) Probing the interior of fullerenes by  $^3\text{He}$  NMR spectroscopy of endohedral  $^3\text{He}@C_{60}$  and  $^3\text{He}@C_{70}$ . *Nature* 367:256–258
- Buhl M, Patchkovskii S, Thiel W (1997) Interaction energies and NMR chemical shifts of noble gases in  $C_{60}$ . *Chem Phys Lett* 275:14–18
- Dodziuk H, Dolgonos G, Lukin O (2001) Molecular mechanics study of endohedral fullerene complexes with small molecules. *Carbon* 39:1907–1911
- Kareev IE, Bubnov VP, Laukhina EE, Koltover VK, Yagubskii EB (2003) Endohedral metallofullerenes  $M@C_{82}$  ( $M=\text{La}, \text{Y}$ ): synthesis and transport properties. *Carbon* 41:1375–1380
- Saunders M, Jiménez-Vázquez HA, Cross RJ, Mroczkowski S, Gross ML, Giblin DE, Poreda RJ (1994) Incorporation of helium,

- neon, argon, krypton, and xenon into fullerenes using high-pressure. *J Am Chem Soc* 116:2193–2194
9. Saunders M, Cross RJ, Jiménez-Vázquez HA, Shimshi R, Khong A (1996) Noble gas atoms inside fullerenes. *Science* 271:1693–1697
  10. Murata Y, Murata M, Komatsu K (2003) 100 % encapsulation of a hydrogen molecule into an open-cage fullerene derivative and gas-phase generation of  $H_2@C_{60}$ . *J Am Chem Soc* 125:7152–7153
  11. Stanisky CM, Cross RJ, Saunders M, Murata M, Murata Y, Komatsu K (2005) Helium entry and escape through a chemically opened window in a fullerene. *J Am Chem Soc* 127:299–302
  12. Komatsu K, Murata M, Murata Y (2005) Encapsulation of molecular hydrogen in fullerene  $C_{60}$  by organic synthesis. *Science* 307:238–240
  13. Stanisky CM, Cross RJ, Saunders M (2009) Putting atoms and molecules into chemically opened fullerenes. *J Am Chem Soc* 131:3392–3395
  14. Balch AL (2011)  $H_2O$  in a desert of carbon atoms. *Science* 333:531–532
  15. Kurotobi K, Murata Y (2011) A single molecule of water encapsulated in fullerene  $C_{60}$ . *Science* 333:613–616
  16. Teligmann R, Krawez N, Lin S, Hertel IV, Campbell EEP (1996) Endohedral fullerene production. *Nature* 382:407–408
  17. Shimshi R, Cross RJ, Saunders M (1997) Beam implantation: a new method for preparing cage molecules containing atoms at high incorporation levels. *J Am Chem Soc* 119:1163–1164
  18. Ohtsuki T, Ohno K, Shiga K, Kawazoe Y, Maruyama Y, Masumoto K (1998) Insertion of Xe and Kr atoms into  $C_{60}$  and  $C_{70}$  fullerenes and the formation of dimers. *Phys Rev Lett* 81:967–970
  19. Patchkovskii S, Thiel W (1996) How does helium get into buckminsterfullerene? *J Am Chem Soc* 118:7164–7172
  20. Zahn D (2005) Unprejudiced identification of reaction mechanisms from biased transition path sampling. *J Chem Phys* 123:44104–44110
  21. Granot R, Baer R (2008) A tight-binding potential for helium in carbon systems. *J Chem Phys* 129:214102–214106
  22. Peng RF, Chu SJ, Huang YM, Yu HJ, Wang TS, Jin B et al (2009) Preparation of  $He@C_{60}$  and  $He_2@C_{60}$  by an explosive method. *J Mater Chem* 19:3602–3605
  23. Manaa MR, Fried LE, Melius CF, Elstner M, Frauenheim T (2002) Decomposition of HMX at extreme conditions a molecular dynamics simulation. *J Am Chem Soc* 106:9024–9029
  24. Dlott DD (1999) Ultrafast spectroscopy of shock waves in molecular materials. *Annu Rev Phys Chem* 50:251–278
  25. Strachan A, van Duin ACT, Chakraborty D, Dasgupta S, Goddard WA III (2003) Shock waves in high-energy materials: the initial chemical events in nitramine RDX. *Phys Rev Lett* 91:98301–98304
  26. Strachana A, Kober EM, van Duin ACT, Oxgaard J, Goddard WA III (2005) Thermal decomposition of RDX from reactive molecular dynamics. *J Chem Phys* 122:54502–54511
  27. Liu L, Krack M, Michaelides A (2008) Density oscillations in a nanoscale water film on salt: insight from Ab initio molecular dynamics. *J Am Chem Soc* 130:8572–8573
  28. Liu LM, Krack M, Michaelides A (2009) Interfacial water: a first principles molecular dynamics study of a nanoscale water film on salt. *J Chem Phys* 130:234702–234713
  29. Vondele JV, Krack M, Mohamed F, Parrinello M, Chassaing T, Hutter J (2005) Quickstep: fast and accurate density functional calculations using a mixed Gaussian and plane waves approach. *Comput Phys Commun* 167:103–128
  30. Perdew JP, Burke K, Ernzerhof M (1996) Generalized gradient approximation made simple. *Phys Rev Lett* 77:3865–3868
  31. Grimme S, Antony J, Ehrlich S, Kriegel H (2010) A consistent and accurate ab initio parametrization of density functional dispersion correction (DFT-D) for the 94 elements H–Pu. *J Chem Phys* 132:154104–154122
  32. Henkelman G, Uberuaga BP, Jonsson H (2000) A climbing image nudged elastic band method for finding saddle points and minimum energy paths. *J Chem Phys* 113:9901–9904
  33. Kabir M, Mukherjee S, Saha-Dasgupta T (2011) Substantial reduction of Stone-Wales activation barrier in fullerene. *Phys Rev B* 84:205404–205410
  34. Hesselmann A, Korona T (2011) On the accuracy of DFT-SAPT, MP2, SCS-MP2, MP2C, and DFT+Disp methods for the interaction energies of endohedral complexes of the  $C_{60}$  fullerene with a rare gas atom. *Phys Chem Chem Phys* 13:732–743
  35. Cao BP, Peres T, Cross RJ, Saunders M, Lifshitz C (2005) Unimolecular dissociations of  $C_{70}^+$  and its noble gas endohedral cations  $Ne@C_{70}^+$  and  $Ar@C_{70}^+$ : Cage-binding energies for  $C_2$  loss. *J Phys Chem A* 109:10257–10263
  36. Cao B, Peres T, Cross RJ, Saunders M, Lifshitz C (2001) Do nitrogen-atom-containing endohedral fullerenes undergo the shrink-wrap mechanism? *J Phys Chem A* 105:2142–2146
  37. Jakowski J, Irlé S, Morokuma K (2010) Collision-induced fusion of two  $C_{60}$  fullerenes: quantum chemical molecular dynamics simulations. *Phys Rev B* 82:125443–125450
  38. Brink C, Hvelplund P, Shen H, Jiménez-Vázquez HA, Cross RJ, Saunders M (1998) Collisional fragmentation of  $Ar@C_{60}$ . *Chem Phys Lett* 286:28–34
  39. Saunders M, Jiménez-Vázquez HA, Cross RJ, Poredaet RJ (1993) Stable compounds of helium and neon:  $He@C_{60}$  and  $Ne@C_{60}$ . *Science* 259:1428–1430

To experimentally study explosion shock wave, a method of small scale gap test was improved to guarantee the steady propagation of shock wave, a Mn–Cu manometer was used to measure the detonation pressure (23.5–28.8 GPa), and the range of detonation velocity was 2 to  $5 \times 10^3$  m  $s^{-1}$ . It was found that there is a close relation between explosion shock wave of explosive quality and the yields of  $He@C_{60}$